Journal of the European Ceramic Society 17 (1997) 735–741
© 1997 Elsevier Science Limited
Printed in Great Britain. All rights reserved
0955-2219/97/$17.00

PII: S0955-2219(96)00083-0

Effect of Sintering Atmosphere on the Mechanical Properties of Ni/Al_2O_3 Composites

W. H. Tuan, H. H. Wu & R. Z. Chen

Institute of Materials Science and Engineering, National Taiwan University, Taipei, Taiwan 10764

(Received 7 August 1995; revised version received 2 April 1996; accepted 3 May 1996)

Abstract

In the present study, nickel-toughened aluminas are prepared by sintering in either hydrogen or carbon monoxide. By choosing suitable sintering temperatures, the size of nickel inclusions is the same in the composites sintered in H_2 *and CO. The addition of nickel inclusions enhances the toughness of alumina. As the inclusion size is bigger than 2·7 μm, microcracks are formed at the interface in the composites sintered in* H_2*. The toughness and strength of the composites are thus reduced. However, no microcracks are observed at the interface in the composites sintered in CO. The toughness and strength of the composites sintered in CO is therefore higher than those of the composites sintered in* H_2*. For example, for the composite containing 20 vol% inclusions and sintered in CO, the toughness is 9 MPa* $m^{0.5}$ *and the strength is 630 MPa. © 1997 Elsevier Science Limited. All rights reserved.*

1 Introduction

Brittle ceramics can be toughened by the incorporation of ductile inclusions.[1–3] The toughness enhancement is mainly contributed by the plastic deformation of metallic inclusions. Two conditions have to be fulfilled in order for the plastic deformation to be fully exploited: (1) to ensure that the crack is attracted by the metallic particles, the elastic modulus of the metal should be lower than that of the ceramic matrix; (2) the metallic particles need to be firmly bonded to the brittle matrix. The size of the inclusions should therefore be kept below the critical size at which thermal mismatch stresses become sufficient to induce cracks.[4] If the ductile inclusion is weakly bonded to the matrix, the crack will propagate along the interface, and the contribution from ductility to the toughening enhancement will be negligible.

Among metals that can be used to toughen alumina, nickel is frequently chosen for its oxidation resistance. Dense Ni/Al_2O_3 composites have been prepared by a powder metallurgy technique,[5] a selective reduction process,[2] a powder coating process[6] and a sol–gel process.[7,8] The reported properties for the composites containing ~13 vol% Ni are shown in Table 1. Some data from the present study are also shown for comparison. These studies indicate that the toughness of alumina can be enhanced by adding nickel inclusions. However, the reported values show a strong dependence on the sintering atmosphere employed. Zhang *et al.* suggested that higher oxygen content in the sintering atmosphere can result in higher toughness.[5] Despite the oxygen content in the sintering atmosphere being varied, no reaction phase at the interface was observed. Chang *et al.* observed no spinel interphase in their Ni/Al_2O_3 composites as well.[9] However, an amorphous carbon film was observed at the interface instead.

The interactions between Al_2O_3 and NiO, Al_2O_3 and Ni have been studied extensively.[10,11] Al_2O_3 reacts with NiO to form $NiAl_2O_4$ spinel above 700°C in air.[10] The spinel can also be formed at Al_2O_3/Ni interfaces as the oxygen solubility in nickel is higher than a threshold value.[11] However, the stability of $NiAl_2O_4$ depends on the oxygen partial pressure in the atmosphere. When the oxygen partial pressure is low, the $NiAl_2O_4$ interphase will eventually reduce to alumina, nickel and oxygen after its formation.[11] In the present study, the effect of sintering atmosphere on the microstructural evolution and toughening behaviour of Ni/Al_2O_3 composites is investigated in detail. Furthermore, the effect of sintering atmosphere on the strength of composites has not been investigated in previous studies. In this study, the effect of sintering atmosphere on the strength is also investigated.

2 Experimental

Alumina (TM-DR, Taimei Chemical Co., Ltd, Tokyo) and various amounts of nickel oxide

Table 1. Reported values for the toughness and strength of nickel-toughened aluminas

Ni content (vol%)	*Size of Ni inclusions (μm)*	*Toughness* $K_{IC,C}/K_{IC,0}$	*Measurement technique for* K_{IC}	*Strength* σ_C/σ_0	*Processing conditions and sintering atmosphere*	*Ref.*
13	1·1	5·0/2·7	ID	—	selective reduction, CO	2
12	20 μm long, 2–3 μm wide	4·1/3·6	SENB	—	powder metallurgy, CO	5
12	20 μm long, 2–3 μm wide	4·9/3·6	SENB	—	powder metallurgy, Ar	5
13	1·1	5·6/4·0	SENB	462/399	powder coating, H_2	6
10	0·02–50	6·3/3·8	ID	—	sol–gel, hot-pressing	7
13	2·7	5·0/3·6	SENB	406/456	selective reduction; H_2	this study
13	2·6	7·5/4·0	SENB	659/317	selective reduction, CO	this study

Notes: $K_{IC,C}$ = fracture toughness of the composite (MPa $m^{0.5}$); $K_{IC,0}$ = fracture toughness of alumina alone (MPa $m^{0.5}$); ID = indentation technique; SENB = single-edge notched beam technique; σ_C = flexural strength of the composite (determined by the four-point bending technique) (MPa); σ_0 = flexural strength of alumina alone (determined by the four-point bending technique) (MPa).

(Johnson Matthey Co., USA) were milled together for 4 h in ethyl alcohol with a turbo-mixer. The powder mixtures would result in 0, 2, 5, 8, 13 and 20 vol% nickel after sintering in a reducing atmosphere. The grinding medium used was zirconia balls. The slurry of the powder mixtures was dried with a rotary evaporator. The dried lumps were crushed and sieved through a plastic sieve. Powder compacts were formed by first uniaxially pressing at 10 MPa, then by isostatic pressing at 250 MPa.

For the composites sintered in flowing hydrogen (H_2), the sintering was performed with a tube furnace. The sintering atmosphere was a mixture of 5% hydrogen and 95% nitrogen. The gas mixture was first passed through concentrated sulfuric acid (H_2SO_4) to reduce the water content. The powder compacts were reduced in hydrogen at 800°C for 50 h, then sintered at 1600°C for 1 h, Fig. 1(a). The sintering atmosphere of carbon monoxide (CO) was generated by arranging specimens in covered graphite crucible. The crucible was then fired in a box furnace. The sintering in CO was performed at 1650°C for 1 h, Fig. 1(b). The sintering temperatures were chosen to result in the same inclusion size for the composites sintered either in H_2 or in CO. The heating and cooling rates were 5°C min^{-1}.

The final density of the composites was determined by a water displacement method. Before submerging the specimens in water, a wax was applied to the surface to prevent water penetration. The polished surfaces were prepared by grinding and polishing with diamond paste to 6 μm and with silica suspension to 0·05 μm. The size of the nickel inclusions after sintering was determined by using the linear intercept technique. The polished specimens were then thermally etched at 1500°C for 1 h in H_2 to reveal the grain boundaries of the matrix. The size of the matrix grains was also determined by using the linear intercept technique. The microstructure of the specimens was observed by scanning electron microscopy (SEM) and transmission electron micro-

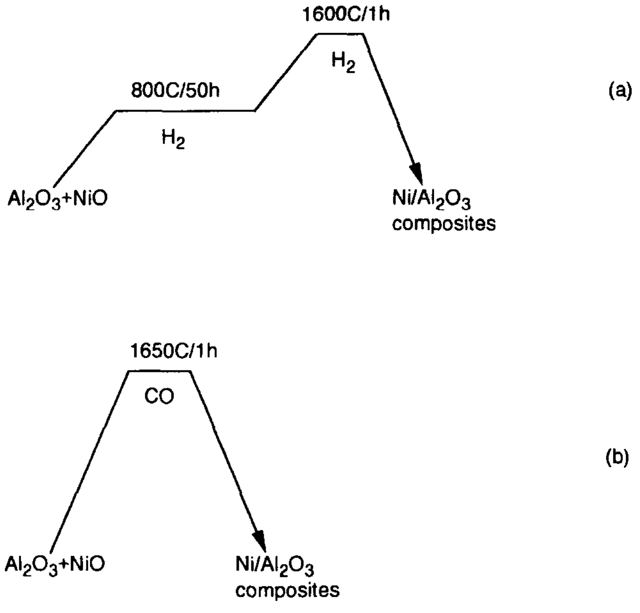

Fig. 1. Sintering profiles for the composites sintered in (a) H_2 and (b) CO.

scopy (TEM). Phase identification was performed by X-ray diffractometry (XRD). Silicon powder was used as internal standard to determine the lattice parameter of nickel.

The sintered composites were machined longitudinally with a 325 grit metal-bonded diamond wheel at cutting depths of 5 μm per pass. The final dimensions of the specimens were 3 × 4 × 36 mm^3. The strength of the specimens was determined by the four-point bending technique. The upper and lower spans were 10 mm and 30 mm, respectively, and the rate of loading was 0·5 mm min^{-1}. The fracture toughness was determined by the single edge notched bean (SENB) technique. The notch was generated by cutting with a diamond saw.

3 Results and Discussion

3.1 Thermodynamic analysis

Passing the gas through concentrated sulfuric acid reduces the water content to 0·003 mg per litre of gas.[12] The partial pressure of oxygen can be estimated with the reaction equation as

$$H_2(g) + \frac{1}{2} O_2(g) = H_2O(g) \qquad (1)$$

At 1600°C, the Gibbs free energy change for the reaction is −140 000 J mol^{-1}.[13] The oxygen partial pressure at 1600°C is therefore 8 × 10^{-17} atm.

At temperatures higher than 700°C, carbon is mainly reacted with oxygen to form carbon monoxide as[14]

$$C(s) + \frac{1}{2} O_2(g) = CO(g) \qquad (2)$$

The Gibbs free energy change for the reaction at 1650°C is −560 000 J mol^{-1}. By assuming unit activity for the solid phase, the equilibrium oxygen partial pressure at 1650°C is 10^{-15} atm.

Nickel melt can react with Al_2O_3 and O_2 to form $NiAl_2O_4$ as

$$Ni(l) + \frac{1}{2} O_2(g) + Al_2O_3(s) = NiAl_2O_4(s) \qquad (3)$$

The Gibbs free energy change for the above reaction between 1500 and 1700°C has been expressed as[15]

$$\Delta G = -241\,800 + 74{\cdot}2\ T \text{ J mol}^{-1} \qquad (4)$$

where T is temperature in K. The equilibrium oxygen pressure for reactions (1), (2) and (3) is shown in Fig. 2. Because the oxygen partial pressure in the sintering atmosphere is much lower than the oxygen pressure needed for reaction (3) to take place, the formation of $NiAl_2O_4$ is not possible.

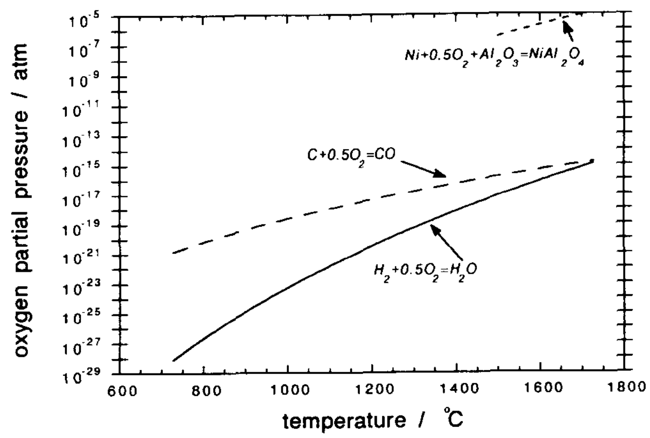

Fig. 2. Oxygen partial pressure during sintering as a function of temperature.

The starting material used in the present study comprises powder mixtures of Al_2O_3 and NiO. As NiO is fully reduced to Ni first at 800°C for 50 h, the formation of $NiAl_2O_4$ during sintering is not possible. As Al_2O_3/NiO powder mixtures are sintered in CO without the pre-sintering stage, $NiAl_2O_4$ can be formed at the beginning of sintering. However, the $NiAl_2O_4$ phase tends to be reduced fully to Al_2O_3 and Ni eventually. In XRD patterns, no $NiAl_2O_4$ spinel was observed in the composites after sintering in H_2 or in CO. Therefore, the XRD results confirm the thermodynamic analysis.

3.2 Sintering and microstructural evolution

For sintering in H_2, the pre-sintering stage is essential to produce a uniform microstructure: sintering the Al_2O_3/NiO powder compacts at 1600°C for 1 h in hydrogen without pre-sintering at 800°C resulted in a non-uniform microstructure. The skin layer of the fired compact is composed of only Al_2O_3 and Ni; however, not only Al_2O_3 and Ni but also $NiAl_2O_4$ are found in the central region. This is due to the densification of the skin layer being faster than the reduction of NiO and $NiAl_2O_4$. When a dense skin layer is formed, the reduction of NiO and $NiAl_2O_4$ is difficult because the diffusion of oxygen through the dense skin is slow. The powder compacts were thus pre-sintered at 800°C for 50 h in H_2 to reduce NiO first. After pre-sintering, neither NiO nor $NiAl_2O_4$ is observed.

For the Al_2O_3/NiO powder compacts sintered in CO at 1650°C, dense Ni/Al_2O_3 composites are obtained without a pre-sintering treatment. To be shown later, the grain size of alumina in the composites sintered in CO is bigger than that in the composites sintered in H_2. The densification rate of the composites sintered in CO is thus slower. The reduction of NiO and $NiAl_2O_4$ can thus be achieved before densification is completed.

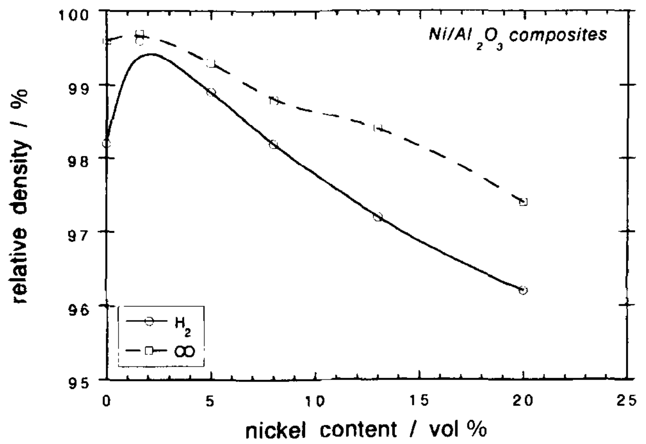

Fig. 3. Relative density of Ni/Al$_2$O$_3$ composites as a function of nickel content.

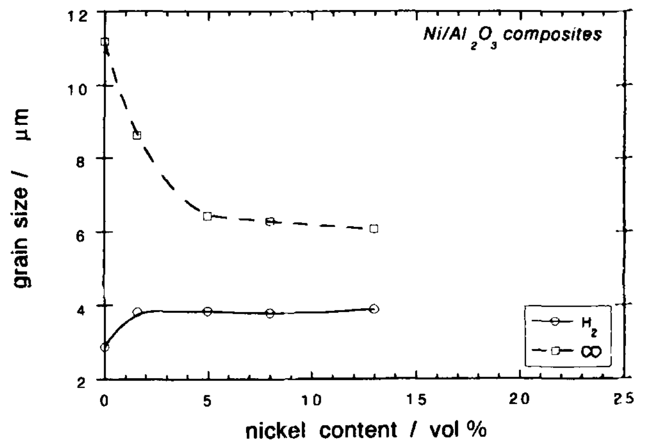

Fig. 5. Size of matrix Al$_2$O$_3$ grains in Ni/Al$_2$O$_3$ composites as a function of nickel content.

The relative density of the composites is shown as a function of nickel content in Fig. 3. The relative density of the composites is greater than 96%. Mehrotra and Chaklader have determined the Al$_2$O$_3$/Ni interfacial energy as a function of oxygen pressure.[16] They suggested that the energy is independent of oxygen pressure at oxygen pressures lower than 10^{-3} atm. The oxygen pressure under investigation in the present study ranges from 10^{-17} to 10^{-15} atm. The Al$_2$O$_3$/Ni interfacial energy is therefore independent of sintering atmospheres used in the present study. The sintering behaviour of Ni/Al$_2$O$_3$ composites in H$_2$ and in CO should be very similar. The density difference for the composites sintered in the different sintering atmospheres is indeed small.

The inclusion size of nickel is shown as a function of nickel content in Fig. 4. The inclusion sizes in the composites sintered in CO and H$_2$ are very close to one another. The toughness enhancement for the ceramic/metal composites depends strongly on the size of the metallic inclusion.[17] The mechanical properties can thus be compared on the same inclusion size and similar density. The effect of sintering atmosphere on the mechanical properties can therefore be identified. The grain size of the alumina matrix is shown as a function of nickel content in Fig. 5. Typical microstructures for the composites are shown in Fig. 6. Because the composites sintered in CO were sintered at higher temperature, the resulting grain size is thus bigger. Furthermore, the Al$_2$O$_3$/NiO powder compacts were fired directly to the sintering tempera-

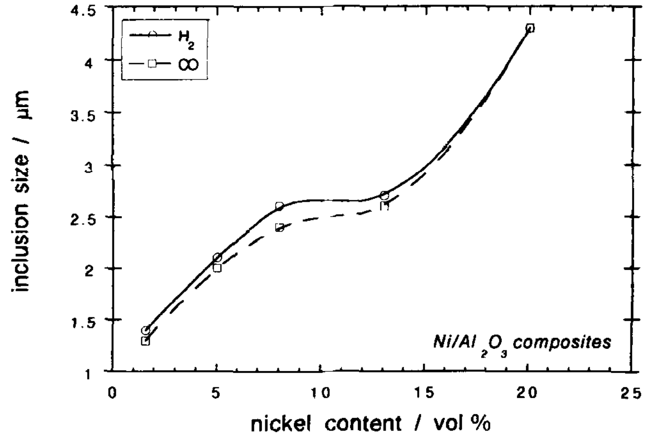

Fig. 4. Size of nickel inclusions in Ni/Al$_2$O$_3$ composites as a function of nickel content.

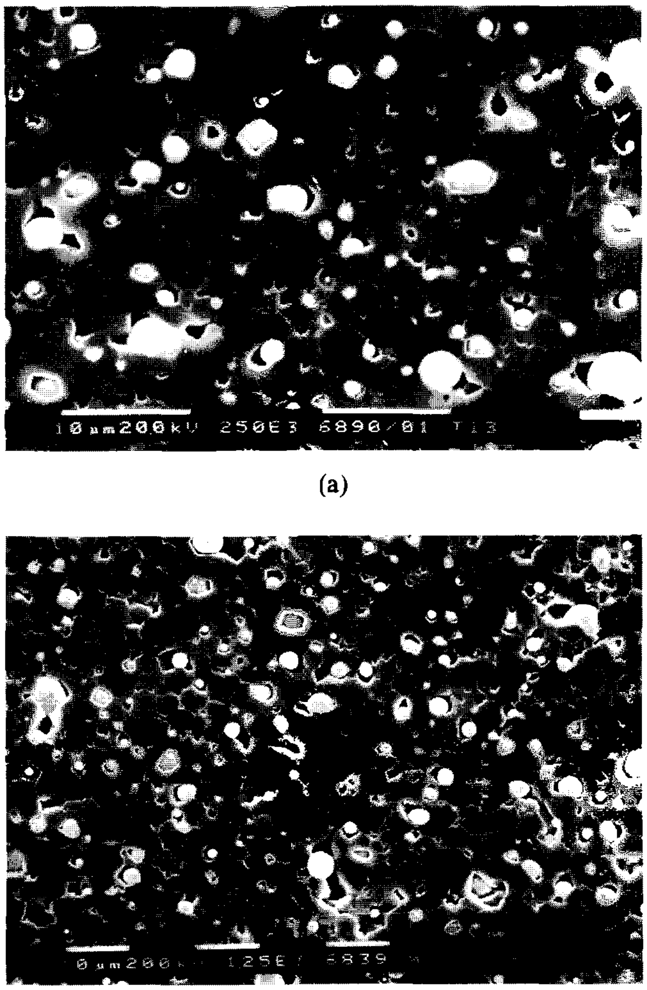

(a)

(b)

Fig. 6. Typical microstructures for the Ni/Al$_2$O$_3$ composites sintered in (a) H$_2$ and (b) CO.

ture in CO. During the heating-up stage, a small amount of nickel oxide can dissolve into alumina. The nickel ions segregate preferentially at the boundaries of alumina,[18] thus refining the matrix grain size. For the composites sintered in H_2, NiO is fully reduced to Ni first. The solubility of metallic nickel in alumina during sintering is limited, and hence the influence of the nickel oxide addition on the grain growth of alumina during sintering in H_2 is small.

3.3 Mechanical properties/microstructure relationships

The flexural strength of the composites is shown as a function of nickel content in Fig. 7. Each point in the figure represents the average value of four specimens, while the error bars indicate the maximum and minimum values measured. The grain size of alumina sintered in H_2 is smaller than that of alumina sintered in CO, thus the strength of alumina sintered in H_2 is higher than that of the alumina sintered in CO. The strength of the composites sintered in CO is significantly higher than that of alumina alone. For example, the strength of the composite containing 20 vol% Ni is 630 MPa, this strength being twice that of alumina alone. As can be seen from Fig. 5, the grain size of alumina decreased with increasing nickel content as the composites were sintered in CO. As the strength of the composites is increased with increasing nickel content, the microstructural refinement contributes to the strengthening effect.

The toughness of the composites is shown as a function of nickel content in Fig. 8. The toughness of alumina is enhanced by adding nickel inclusions. Microstructural observation shows, similar to the previous studies,[1-6] that the toughness enhancement is contributed by crack bridging and crack deflection. The highest toughness value observed in the present study is 9 MPa $m^{0\cdot5}$, which is 2·3 times that of alumina alone, for the composite containing 20 vol% Ni and sintered in CO. However, the toughness of the composites sintered in H_2 increased only slightly and the toughness dropped at Ni contents higher than 13 vol%. At that Ni content, the corresponding nickel size is 2·7 μm. Several composites were used for TEM observation. No second phase was observed at the interface in the composites sintered in H_2 or in CO, Fig. 9. However, microcracks were observed at the interface of the composites sintered in H_2. Even within one specimen, microcracks were observed only at the interface with inclusions larger than 2·7 μm. One example is shown in Fig. 9(a). For composites sintered in CO, after careful observation of several specimens, no microcrack was observed at the interface. An example is shown in Fig. 9(b). Despite the inclusion size in Fig. 9(b) being larger than 4 μm, no microcrack is present at the interface.

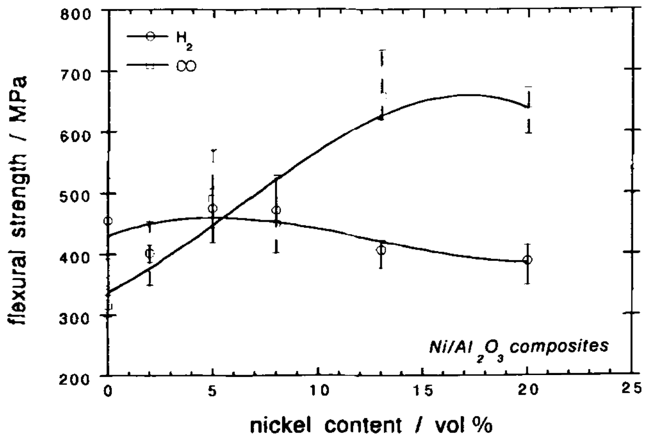

Fig. 7. Flexural strength of Ni/Al_2O_3 composites as a function of nickel content.

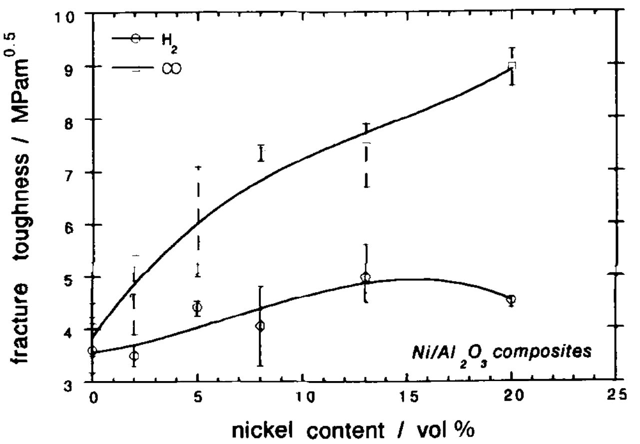

Fig. 8. Fracture toughness of Ni/Al_2O_3 composites as a function of nickel content.

The presence of microcracks deviates the propagation of cracking. However, the contribution from crack deflection around spherical particles to toughness enhancement is limited.[19] As Ni inclusions are firmly bonded to the matrix, the plastic deformation of nickel inclusions is then possible. The toughness can be enhanced significantly by the plastic deformation of the ductile inclusions. The presence of microcracks degrades the strength of ceramics. At nickel contents of 13 vol% Ni, the strength of the composites sintered in H_2 dropped whereas the strength of composites sintered in CO increased with increasing nickel content. This results from grain refinement and the absence of microcracks.

Chang *et al.* sintered their Ni/Al_2O_3 composites using a graphite powder bed,[9] and amorphous carbon was found at the interface. In the present study, attempts to locate the carbon film at the interface were not successful. However, carbon from the sintering atmosphere can dissolve in nickel at high temperature. This has been confirmed by measurement of the lattice parameter of nickel. The lattice parameter of nickel in the

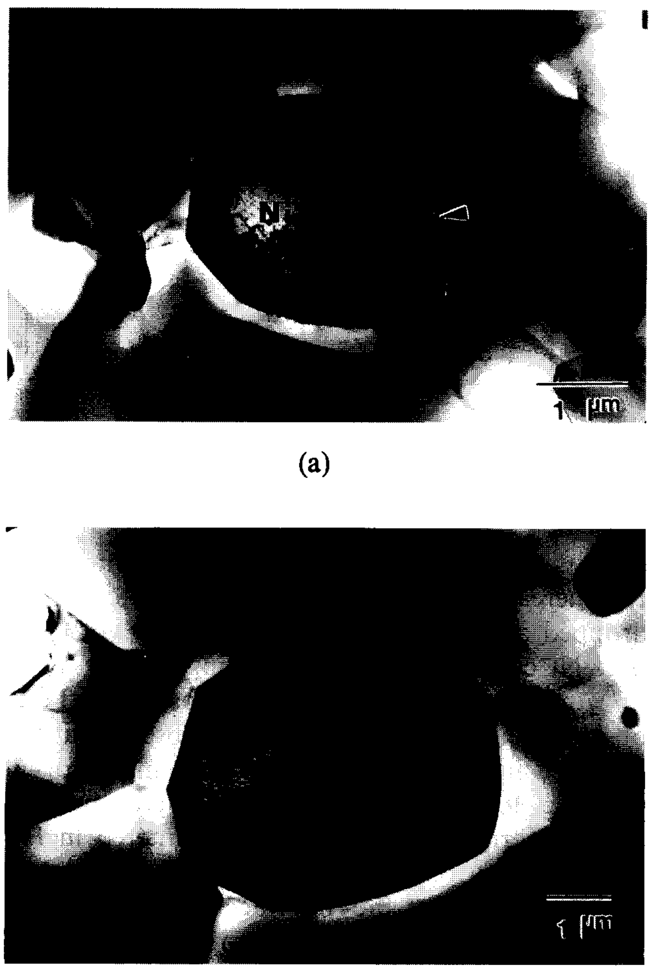

(a)

(b)

Fig. 9. TEM micrographs of the Ni/Al_2O_3 composites sintered in (a) H_2 and (b) CO. The microcrack is indicated with an arrow.

composite sintered in CO is 2·036 Å, which is higher than the reported JCPD value (2·034 Å), suggesting that carbon is dissolved in nickel during sintering. The reported properties[20] for pure nickel and nickel containing a small amount of carbon are shown in Table 2. As can be seen, the presence of carbon has little effect on the thermal expansion coefficient, elastic modulus and hardness. However, the yield strength of nickel is significantly increased as the carbon content is increased. The toughness increase due to the addition of a ductile inclusion is proportional to its yield strength.[17] The toughness enhancement of the composites sintered in CO is thus higher.

The thermal expansion of nickel (13 μm/m K) is higher than that of alumina (9 μm/m K); the Al_2O_3/Ni interface is thus subjected to a radial tensile stress as the composite cools from the firing temperature. As the yield strength is higher, the metallic inclusion is more difficult to deform plastically upon cooling. The Al_2O_3/Ni interface may thus be intact upon cooling. Plastic deformation of the ductile inclusions during the subsequent fracture process is therefore possible. The toughness is enhanced significantly due to the plastic deformation of nickel inclusions and the absence of microcracks.

4 Conclusions

In the present study, Ni/Al_2O_3 composites were sintered in hydrogen or in carbon monoxide and the effect of sintering atmosphere on the mechanical properties of the Ni/Al_2O_3 composites investigated. The composites were sintered in CO at 1650°C or in H_2 at 1600°C. After sintering, no $NiAl_2O_4$ spinel is formed at the interface. The density and the inclusion size of the resulting composites are very similar. In composites sintered in CO a small amount of carbon dissolved into the nickel, thus increasing the yield strength of the nickel inclusion. The toughness of the composites sintered in CO is thus higher. Furthermore, because the yield strength is high, the nickel inclusion is not easily deformed plastically upon cooling. The Al_2O_3/Ni interface remains stable, and microcracks were not observed at the interface in the composites sintered in CO. The toughness and strength of the alumina are therefore significantly enhanced. However, microcracks are observed in the composites sintered in H_2. The toughness enhancement of the composites is thus low, as is the strength of the composites.

Acknowledgement

This work was supported by the National Science Council, Republic of China, through contract number NSC83-0405-E002-014.

Table 2. Reported properties for pure nickel and nickel containing a small amount of carbon[20]

Materials	*Carbon content (wt%)*	*Linear thermal expansion (μm/m K)*	*Elastic modulus (GPa)*	*Hardness*	*Yield strength (MPa)*
Nickel 200[a]	0·15	13·3	204	109 HB	148
Nickel 201[b]	0·02	13·1	207	129 HB	103

[a] Composition = 99·0% Ni(min), 0·25% Cu, 0·40% Fe, 0·35% Mn, 0·15% C, 0·35% Si, 0·01% S.
[b] Composition = 99·0% Ni(min), 0·25% Cu, 0·40% Fe, 0·35% Mn, 0·02% C, 0·35% Si, 0·01% S.

References

1. Aghajanian, M. K., MacMillan, N. H., Kennedy, C. R., Luszcz, S. J. & Roy, R., Properties and microstructures of Lanxide Al_2O_3–Al ceramic composite materials. *J. Mater. Sci.*, **24** (1989) 658–670.
2. Tuan, W. H. & Brook, R. J., The toughening of alumina with nickel inclusions. *J. Eur. Ceram. Soc.*, **6** (1990) 31–37.
3. Chou, W. B. & Tuan, W. H., Toughening and strengthening alumina with silver inclusions. *J. Eur. Ceram. Soc.*, **15** (1995) 291–295.
4. Davidge, R. W. & Green, T. J., The strength of two-phase ceramic/glass materials. *J. Mater. Sci.*, **3** (1968) 629–634.
5. Zhang, X., Lu, G., Hoffmann, M. J. & Metselaar, R., Properties and interface structures of Ni and Ni–Ti alloy toughened Al_2O_3 ceramic composites. *J. Eur. Ceram. Soc.*, **15** (1995) 225–232.
6. Tuan, W. H., Wu, H. H. & Yang, T. J., The preparation of Al_2O_3/Ni composites by a powder coating technique. *J. Mater. Sci.*, **30** (1995) 855–859.
7. Breval, E., Deng, Z., Chiou, S. & Pantano, C. G., Sol–gel prepared Ni-alumina composite materials, part 1, microstructure and mechanical properties. *J. Mater. Sci.*, **27** (1992) 1464–1468.
8. Rodeghiero, E. D., Tse, O. K. & Giannelis, E. P., Interconnected metal–ceramic composites by chemical means. *J. Metal*, **47** (1995) 26–28.
9. Chang, L., Chen, S. C., Tuan, W. H. & Brook, R. J., Interfacial characterization of Al_2O_3/Ni composites. *J. Eur. Ceram. Soc.*, **12** (1993) 479–486.
10. Simpson, Y. K., Colgan, E. G. & Carter, C. B., Kinetics of the growth of spinel on alumina using Rutherford backscattering spectroscopy. *J. Am. Ceram. Soc.*, **70** (1987) C-149–C-151.
11. Trumble K. P. & Ruehle, M., The thermodynamics of spinel interphase formation at diffusion-bonded Ni/Al_2O_3 interfaces. *Acta Metall. Mater.*, **39** (1991) 1915–1924.
12. Yoe, J. H., Efficiency of drying agents. In *CRC Handbook*, 58th edn, ed. R. C. Weast. CRC Press, Florida, 1978, p. E-22.
13. Daniels, F. & Alberty, R. A. In *Physical Chemistry*, 4th edn. John Wiley & Sons, Inc., New York, 1975, p. 178.
14. SGTE Substance Data File, Thermodata GmbH, Grenoble University, St. Martin d'Heres, France, 1987.
15. Jacob, K. T., Solubility and activity of oxygen in liquid nickel in equilibrium with α-Al_2O_3 and NiO $(1+x)$ Al_2O_3. *Metall. Trans.*, **17B** (1986) 763–770.
16. Mehrotra, S. P. & Chaklader, A. C. D., Interfacial phenomena between molten metals and sapphire substrate. *Metall. Trans.*, **16B** (1985) 567–575.
17. Ashby, A. F., Blunt, F. J. & Bannister, M., Flow characteristics of highly constrained metal wires. *Acta Metall.*, **37** (1989) 1847–1857.
18. Jorgensen, P. J. & Westbrook, J. H., Role of solute segregation at grain boundaries during final-stage sintering. *J. Am. Ceram. Soc.*, **47** (1964) 332–338.
19. Faber, K. T. & Evans, A. G., Crack deflection processes — I, theory. *Acta Metall.*, **31** (1983) 565–576.
20. Mankins, W. L. & Lamb, S., Nickel and nickel alloys. In *Metals Handbook*, 10th edn. ASM International, OH, 1990, vol. 2, pp. 428–445.